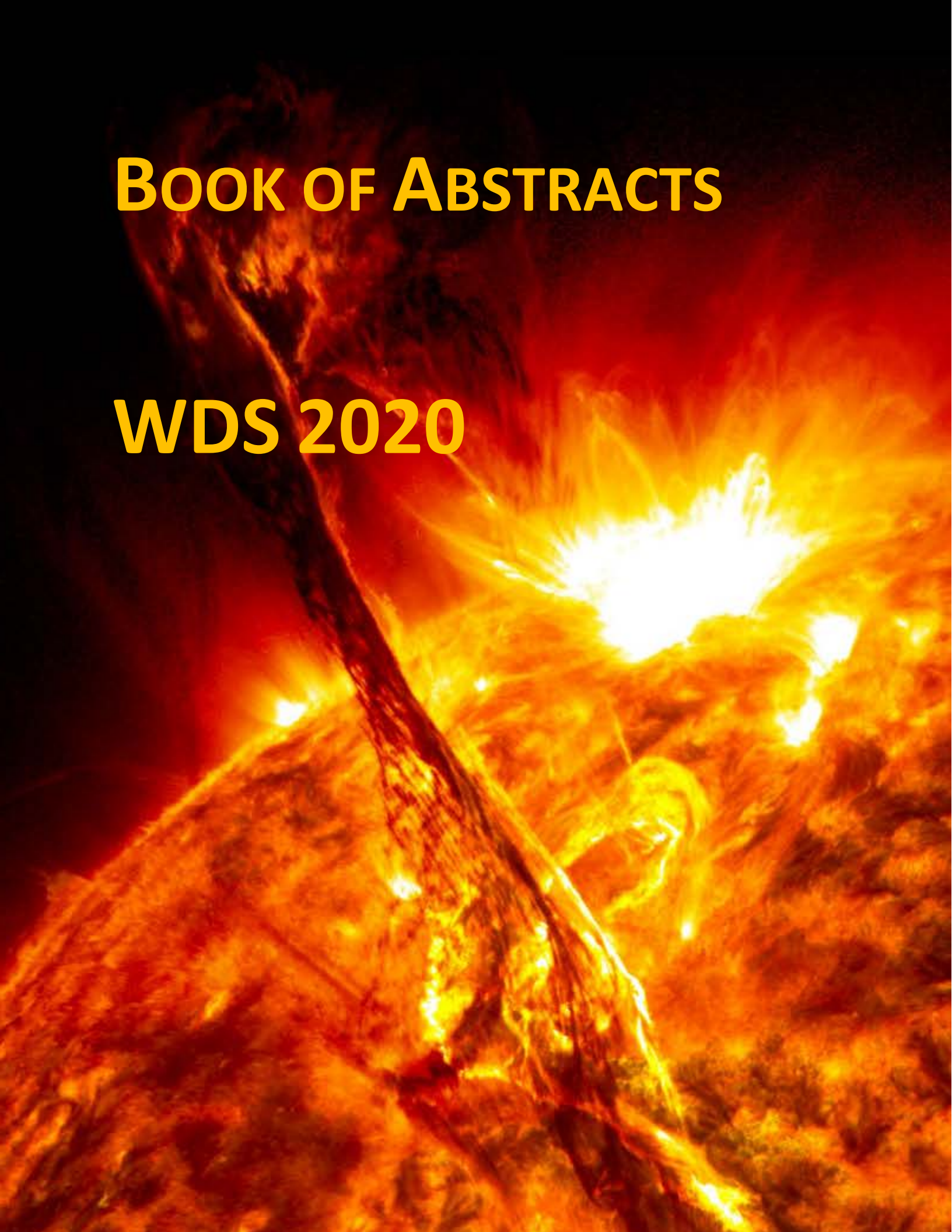


# **BOOK OF ABSTRACTS**

**WDS 2020**





# BOOK OF ABSTRACTS

Week of Doctoral Students 2020

Prague, September 22–24, 2020

© J. Šafránková and J. Pavlů (editors), 2020

---



# CONTENTS

Abstracts are listed alphabetically  
by presenting authors in each section.

f-1 Theoretical Physics, Astronomy and Astrophysics .....	7
f-2 Physics of Plasma and Ionized Media .....	12
f-3 Physics of Condensed Matter and Material Research .....	21
f-4 Biophysics, Chemical and Macromolecular Physics.....	24
f-5 Physics of Surfaces and Interfaces .....	29
f-6 Quantum Optics and Optoelectronics.....	32
f-9 Particle and Nuclear Physics.....	34
f-11 Mathematical and Computer Modelling.....	36
f-12 Physics Education and General Problems of Physics.....	37
f-13 Physics of Nanostructures.....	38



## F-1 THEORETICAL PHYSICS, ASTRONOMY AND ASTROPHYSICS

### Candidates for Proto-Planetary Nebulae Among Stars Exhibiting the B[e] Phenomenon

***Dvořáková N.***

**Abstract.** The B[e] type stars are known for complex emission spectra. They are heavily obscured by an extended envelope of dust and gas as evidenced by a large quantity of forbidden lines of metals present in the spectra. Our main focus is on stars in the post-AGB phase which is still not completely understood. This phase however links the asymptotic giant branch stars and planetary nebulae. We aim to improve our understanding of these objects using spectral diagnostics and the CLOUDY ionization code.

### Elliptical Galaxies in MOND

***Eappen R. and Kroupa P.***

**Abstract.** Fully self-consistent simulations of the formation of elliptical galaxies in the early Universe are performed assuming no dark matter. The idea is to start with a post-Big Bang pre-galactic gas cloud, allow it to collapse under self-gravity thereby following the star formation history and chemical enrichment. To this end, the RAMSES [Teyssier, 2002] adaptive mesh-refinement code is used and the aim is to include in it the algorithms for calculating the galaxy-wide IMF as pioneered by Ploekinger *et al.* [2014] to allow the collapsing system to self-regulate with a galaxy-wide evolving IMF. This has never been done before. Phantom of Ramses (POR) [Lughausen *et al.*, 2015] is a customized version of RAMSES and includes all its features but uses Milgromian dynamics [Milgrom, 1983]. The aim is to compare these theoretical results with the empirical downsizing results obtained previously [Thomas *et al.*, 2010; Yan *et al.*, 2019] to infer the allowed initial conditions, given the observed properties of elliptical galaxies.



## Schwarzschild Black Hole Encircled by a Rotating Thin Disc: Perturbative Solution

**Kotlařík P.**

**Abstract.** In the talk, we present some of the properties of the perturbative solution describing a rotating light thin disc around the Schwarzschild black hole. After examining the basic parameters of the system, we focus on those properties which demonstrate how the disc gravity influences the geometry of the black hole and those of circular equatorial geodesics.

## Cuts in 2+1 Dimensional AdS Spacetime

**Lukeš P.**

**Abstract.** As exemplified by the BTZ black hole, 2+1 dimensional vacuum AdS spacetime can be turned into black hole spacetime only by cutting along some coordinate lines and identifying the surfaces of this cut. This result supports analytical expansion to non-black-hole massive spacetimes. And to define global mass of AdS tends to be problematic due to nonzero cosmological constant. This poster summarizes currently available results about 2+1 AdS spacetimes and briefly explains the relation of our work to these former results.

## Spectroscopic Analysis of Selected Symbiotic Candidates

**Merc J., Gális R., Wolf M.**

**Abstract.** Symbiotic stars belong to an interesting group of interacting binaries that display a wide variety of phenomena including prominent outbursts connected with mass transfer, stellar winds, and jets, eclipses, or intrinsic variability of the components. Several dozens of new symbiotic stars and candidates have been discovered in recent years. However, there are many objects, which are still poorly studied. In this contribution, we present the first results of the ongoing campaign focused on symbiotic candidates that have never been observed spectroscopically. Some of the targets proved to be symbiotics, others are probably red dwarfs, single subgiants, or giants. We discuss their photometric and spectroscopic properties in detail.





## Study of the White-light Emission During the X9.3 Flare on September 06, 2017

*Mravcová L., Kašparová J., Švanda M., Jurčák J., Heinzel P.*

**Abstract.** In our research, we study the emission in the white light continuum known as the white-light flares. We focused on the X9.3 flare from September 06, 2017, which was the strongest flare in the solar cycle. We used data provided by SDO/HMI to detect the emission. These observations show an excess in a reconstructed pseudo-continuum that should correspond to the Paschen continuum. The flare was also observed by the instrument LYRA, which shows emission in the Balmer continuum. There is a supposed relationship between the emission in the Balmer and the Paschen continuum. The aim of our study is to compare these two emission types and test whether that relation and its assumptions are valid under solar flare conditions.

## Spatiotemporal Correlation Between Gamma-ray Bursts and Ultra-high Energy Neutrinos

*Tarnopolski M., Neporozhni I.*

**Abstract.** In this study we searched for coincident arrivals between photons from gamma-ray bursts (GRBs) and Ultra-High Energy Neutrinos (UHENs). In our work we use data from Fermi-GBM, Swift-BAT and -XRT, and IceCube Observatory. We developed a python program to perform the spatiotemporal cross-match of the compiled datasets that contained 164 UHENs and 3221 GRBs. As a result, 20 GRB-neutrino matches were obtained. The statistical analysis of the results was conducted.

## Searching for Signatures of Chaos in Gamma-ray Light Curves of Selected Fermi/LAT Blazars

*Ostapenko O., Tarnopolski M.*

**Abstract.** The aim of this work was to search for evidence of chaos in 11 well-known blazars, including 3C 279, mkn421 and mkn501. The data were investigated using the phase-space reconstruction and maximal Lyapunov exponent (MLE). The analysis of the object 3C 279 gave convincing results. Outcomes of all performed tests indicated the presence of chaos in this blazar. Value of the MLE is 0.01 (Lyapunov time is 100 days). The rest of the investigated sources did not show clear evidence of chaotic behavior.

## Model-independent Constraints in Inflationary Magnetogenesis

*Shtanov Yu. V., Pavliuk M. V.*

**Abstract.** We derive a simple model-independent upper bound on the strength of magnetic fields obtained in inflationary and post-inflationary magnetogenesis taking into account the constraints imposed by the condition of weak coupling, back-reaction and Schwinger effect. This bound turns out to be rather low for cosmologically interesting spatial scales. Somewhat higher upper bound is obtained if one assumes that some unknown mechanism suppresses the Schwinger effect in the early universe.

## Gravitational Wave Templates from Extreme Mass Ratio Inspirals

*Skoupý V., Loukes-Gerakopoulos G.*

**Abstract.** An extreme mass ratio inspiral takes place when a compact stellar object is inspiraling into a supermassive black hole due to gravitational radiation reaction. Gravitational waves (GWs) from this system can be calculated using the Teukolsky equation (TE). In our case, the asymptotic GW fluxes of a spinning body orbiting a Kerr black hole are computed by solving numerically the TE both in time and frequency domain. The goal is to produce GW templates for space-based detectors such as LISA.

## A Gappy Accretion Disc: Theoretical Profiles of a Relativistic Spectral Line

*Štolc M., Karas V., Zajaček M., Suková P., Witzany V.*

**Abstract.** Stars passing around supermassive black holes can be tidally damaged when reaching the critical distance. It is difficult to distinguish the tidal disruption events (TDEs) in the quiescent galaxy rather than in the active galactic nucleus (AGN). In this paper we consider the effect of a gap in the accretion disc, which can develop due to an embedded star orbiting just above the critical radius for tidal disruption. We model and study its influence on the relativistic spectral line profiles.



## Magnetospheric Response to Solar Wind Driving

*Výboštoková T., Němeček Z.*

**Abstract.** Interaction of solar activity events propagating throughout interplanetary space with the magnetic field of the Earth results in immediate disruption of the magnetosphere. We are studying the relationship between the effect of interplanetary shock and conditions in the Earth's magnetosphere. We investigate 29 different shocks between the years 2009 and 2019. Driving of the magnetosphere is described as integral of the interplanetary magnetic field measured at L1 for each event in 48-hour intervals. The main goal of this study is to suggest a simple algorithm for prediction of the magnetosphere state represented by SYM-H from upstream observations. Comparing in situ measurements of the magnetic field and solar wind speed measured on Wind, integral of z component magnetic field multiply with x component of solar wind speed and SYM-H index are compared on the same time scales for different integration times. There is a strong anti-correlation between the state of the magnetosphere and SYM-H behaviour with time lag ranges between several minutes to 2 hours. With present results, we are on a way to determine a proportion between directly driven and spontaneous magnetosphere response.

## F-2 PHYSICS OF PLASMA AND IONIZED MEDIA

### Overview of the COMPASS-U Cryogenic System Design

*Barton P., Fukova S., Hromadka J., Patočka K., Veselovsky V., Varju J., Havlicek J., Hron M., Panek R.*

**Abstract.** COMPASS-U will be a new tokamak located at IPP Prague. Currently in the construction, it will employ several unique features compared to other tokamaks: toroidal field of intensity up to 5 T, flexible possibilities of plasma shaping, advanced divertor configurations, up to 2 MA plasma current and 2 second flat top plasma duration. To achieve this, copper coils of COMPASS-U will be cooled to 80 K using gaseous helium. Such set of operational parameters define a unique and complex problem for design of an efficient cryogenic system. COMPASS-U will be enclosed in a vacuum cryostat to allow for the use of multilayer insulation (MLI). This allows the tokamak to have a very low steady state heat loss of around 5 kW. To achieve a tokamak discharge repetition frequency of 2 per hour a total cooling power of 200 kW at 80 K is necessary. Solutions employed in the COMPASS-U have not yet been employed in any other tokamak, like all inorganic MLI blankets. In this contribution we present the main features of the design of the cryogenic system.

### Dependence of Properties of Magnetospheric Line Radiation and Quasiperiodic Emissions on Solar Wind Parameters and Geomagnetic Activity

*Bezděková B., Němec F., Parrot M., Hajoš M., Santolík O.*

**Abstract.** Very low frequency electromagnetic waves in the inner magnetosphere can exhibit either frequency or time modulation. These phenomena are called, respectively, magnetospheric line radiation (MLR) and quasiperiodic (QP) emissions. Measurements of these phenomena by the low altitude spacecraft DEMETER were used to analyze their properties, such as MLR frequency spacing, QP modulation period, and QP intensity as functions of geomagnetic activity and solar wind parameters. Altogether, 1,152 MLR events and 2,172 QP emissions were analyzed.



## Direct Determination of Midplane Background Neutral Density Profiles from Neutral Particle Analyzer

***Bogár K., Geiger B., Schneider P. A., Jansen van Vuuren A., Grover O., the ASDEX Upgrade team and the EUROfusionMST1 team***

**Abstract.** Here we present a new method that allows the determination of background neutral density profiles based on measurements from neutral particle analyzers (NPA). Bayesian optimization is used to obtain a reliable 5-parameter representation of the inferred profiles. The method has been benchmarked using forward modelling from FIDASIM. The systematic errors coming from assumptions made in the analysis were evaluated and they are lower than  $\lesssim 5\%$ . The new method has been tested using data from the ASDEX Upgrade tokamak. When using reconstructed neutral density profiles, good agreement is found between the measured NPA fluxes of neutralized fast ions with predictions based on TRANSP and FIDASIM. Moreover, a clear drop of neutral density is observed at the plasma boundary after edge localized mode (ELM) activity. As suggested by KN1D simulations, this drop is mainly due to an increase of scrape of layer (SOL) ionization rate, resulting from higher SOL plasma densities and temperatures after the ELM crash. Moreover the new method allows calculating the local plasma ionization source which will be important for future transport studies.



## Study of the Connection Between the Proton Beam and Alpha Particles in the Solar Wind

*Ďurovcová T., Šafránková J., Němeček Z.*

**Abstract.** Due to turbulent and weakly collisional nature of the solar wind, the ion velocity distribution function of the solar wind shows deviations from the thermodynamic equilibrium. For a given ion species, it can be described by a combination of two bi-Maxwellian populations, a denser dominant core and a minor beam. The relative proton beam abundance is usually between 10% and 20 % and the proton beam is about a local Alfvén speed faster than the proton core. We study a connection between the alpha particle properties and proton beam variations. We found that the relative content of alpha particles is correlated with the relative proton beam abundance, and this effect is more pronounced in the fast solar stream. Since this fast wind is expected to come from coronal holes, the connection between the alpha particles and proton beam could carry an information about the solar wind acceleration mechanisms or put constraints on the interplanetary origin of the proton beam. Using the plasma data measured in-situ in the inner heliosphere (Helios, Wind), we focus on the proton beam development with a radial distance from the Sun as well as on variations during the solar cycle.

## Effective Kinetic Monte Carlo Algorithm for Simulations of Pulsed-Laser Deposition of Layer-by-Layer Growth

*Gabriel V., Kocán P.*

**Abstract.** The main challenge of pulsed-laser deposition (PLD) growth simulations is given by a disparity between short time scales of processes on surface and long times between pulses. We present an efficient kinetic Monte Carlo algorithm in which diffusion is approximated by 2D gas on each layer. The model is suitable for simulations of PLD growth of thin films in range from high to low-frequency cases and it is able to reproduce time evolution of layer coverages observed during the growth.



## **A New Method for Separation of Electrons and Protons in a Space Radiation Field with a Timepix3 Based Radiation Monitor**

***Gohl S., Nemeč F.***

**Abstract.** A Minimized Radiation Monitor (MIRAM) is developed by the Institute of Experimental and Applied Physics, CTU in Prague and ADVACAM s.r.o. The device is supposed to monitor the radiation environment of mainly commercial satellites and works autonomously. It features a Timepix3 pixel detector and four diodes with the power consumption being limited to 1 W. A method was developed to measure the radiation level and to give an estimation of the electron and proton flux without the need of a lot of processing power. The average energy per pixel and the number of hit pixels over a few hundred milliseconds are recorded. A simulation showed that the average energy per pixel for a certain mixture of protons and electrons has a nearly constant value with very little variation at sufficiently high amount of hits regardless of the number of hit pixels. The method was tested on space data from SATRAM, which features a Timepix detector. While lacking the capabilities of its successor, it was shown that the radiation field around the polar regions consist of nearly 100 % of electrons. The proton content of the South Atlantic Anomaly is about 5 to 20 % and while the electron content is 80 to 95 %.

## **Sawtooth Instability and Its Effect on Edge Plasma Processes at COMPASS**

***Imrisek M., Weinzettl V., Tomeš M., Hron M.***

**Abstract.** Sawtooth instability is present in most of the COMPASS experiments where it repetitively fattens the temperature profile in the plasma core. However, it can also influence various processes occurring near the edge of the confined plasma. Statistics of these processes have been recently improved. The main focus of the contribution is the effect of the sawtooth instability on edge localized mode and transition to and from high confinement mode.

## Diagnosics of Surfatron-Generated Plasma in PE-ALD Deposition System

***Kapran A., Hubička Z., Čada M., Tichý M.***

**Abstract.** We present the diagnostic results of surfatron-generated plasma at different experimental conditions: chamber pressure, distance between the RF probe and the nozzle exit. The surfatron is a microwave plasma source for the ignition of surface-wave-sustained discharges. We used commercial surfatron (Sairem) and microwave generator with the maximum power of 1200 W. The characteristics of the generated plasma showed that the surfatron plasma source can generate low-temperature plasma in pressure ranging from 1 Pa up to 200 Pa. Mixtures of Ar (carrier gas), N<sub>2</sub> and O<sub>2</sub> (reactive gases) were used. The diagnostics of plasma was performed by means of Sobolewski probe measurement and optical emission spectroscopy.

## JOREK Simulation of Strike Point Splitting Induced by HFS Magnetic Perturbations on the COMPASS Tokamak

***Kripner L., Becoulet M., Komm M., Markovic T., Peterka M., Fabien J., Adámek J., Tskhakaya D., Pánek R.***

**Abstract.** Strike point splitting has been observed with a delay on the COMPASS tokamak after application of HFS on + off-midplane magnetic perturbation coil configuration. Similar behaviour is attempted to simulate with the non-linear MHD code JOREK. Calculated magnetic footprints are not in a good agreement with probe observation.

## Detection of Specific Volatile Hydrides in Atomizers

***Lacko M., Spanel P., Kratzer H., Matousek T., Dedina J.***

**Abstract.** A popular method for trace element analysis of several elements (As, Se, Sb, Sn, ...) is generation of volatile hydrides. These are produce form an analyte in the liquid phase using the reaction between tetrahydridoborate(-1) (TBH) and acid. The analyte is during the reaction released into gaseous phase where it can be detected by various techniques. SIFT-MS is a powerful analytical method capable of online trace analysis of various volatile species. Thus, we used SIFT-MS to monitor generation of various volatile hydrides and their atomisation in thermal and DBD atomizers.



## Edge Localized Mode Control with 3D Fields in a COMPASS Tokamak

*Markovic T., Peterka M., Weinzettl V., Bogar K., Komm M., Jaulmes F., Bogar O., Kovarik K., Sos M., Tomes M., et al*

**Abstract.** Transport barrier that forms in an H-mode plasma of a tokamak increases its particle confinement time by a factor 2. However, this is accompanied with undesired Edge Localized Mode (ELM) instabilities. The most successful method to control ELM bursts is via 3D perturbation of tokamak confinement field. This work reports on results of ELM control experiments with varying spatial spectra of the 3D perturbations on tokamak COMPASS and interprets them with MHD modelling.

## Current Flows Towards the Divertor During VDEs at COMPASS

*Matveeva E., Havlicek J., Artola F.J., Lehnen M., Pitts R., Roccella R., Dejarnac R., Jerab M., Sestak D., Barton P., Adamek J., Bousek M., Cavalier J., Havranek A., Pova F., Weinzettl V.*

**Abstract.** Determination of vessel currents magnitudes and paths in tokamaks plays crucial role in understanding of mechanical loads on the machine. Two special divertor tiles have been installed on COMPASS tokamak in order to directly measure current flows during vertical displacement events (VDEs). The experiment aims to validate asymmetric toroidal eddy currents (ATEC) model and understand current path within vessel structure and the divertor.

## Perpendicular Measurements of Excited Particles Concentration in DC Glow Oxygen Discharge

*Moravek M.J., Kanka A., Hrachova V.*

**Abstract.** In our studies of DC Glow Discharge in pure oxygen and in oxygen nitrogen mixture we utilized optical emission spectroscopy to measure the concentration of excited species perpendicularly to the discharge axis. Clear distinction between the so-called T- and H-form of the positive column as well as the transitional region are described. Higher concentration of excited oxygen atoms is connected to lower electron concentration determined using toroidal resonator.

## Dynamic Study of Fast Measurement with Langmuir Probe

*Palacky J., Roucka S.*

**Abstract.** Probe measurement is one of the main techniques used to determine the plasma parameters, which are crucial to understand the plasma behaviour. There are many types of probes and the interpretation of the measurements can be very difficult. However, we aim to study the common Langmuir probes, where the determination of plasma parameters from volt-ampere characteristics is well understood under standard conditions. In the data analysis, it is assumed that the probe and the surrounding plasma are always in a steady state. This is easy to achieve with slow measurement, but if there is a need for fast data acquisition, we don't have a certain answer to what is the lowest possible time of measurement. We use a 2D3V particle-in-cell model of a cylindrical Langmuir probe to study the dynamic processes caused by a change of the probe potential. Our aim is to determine the stabilization time needed for fast measurements as a function of plasma parameters and probe potential.

## Ion Trap Study of the Production of OH<sup>+</sup> and OD<sup>+</sup> in the O<sup>+</sup> + HD Reaction

*Rednyk S., Roučka Š., Kovalenko A., Tran T. D., Plašil R., Glosík J.*

**Abstract.** In the present work, the O<sup>+</sup> + HD reaction has been studied using a linear rf 22-pole ion trap. The reaction rate coefficients and the branching ratios for the production of OH<sup>+</sup> and OD<sup>+</sup> were measured in the temperature range from 300 K down to 10 K. The overall reaction rate coefficient at 200 K is  $(1.4 \pm 0.3) \times 10^{-9}$  cm<sup>3</sup>/s. The obtained data are consistent with reaction cross-sections measured in ion-beam experiments.

## Two-point Observations of ULF Fluctuations in the Foreshock

*Salohub A., Šafránková J., Němeček Z., Pi G., Němec F.*

**Abstract.** The foreshock filled with a turbulent plasma is located in upstream Earth's bow shock region where interplanetary magnetic field (IMF) lines are connected to the bow shock surface. In this region, ultra-low frequency (ULF) waves are created due to the interaction of the solar wind plasma with particles reflected from the bow shock back into the solar wind. It is assumed that excited waves growth and they are connected through the solar wind/foreshock, thus the inner spacecraft (close to bow shock) would observe larger wave amplitudes than the outer (far from bow shock) one. The paper presents an analysis of excited ULF fluctuations observed simultaneously by two closely separated ARTEMIS spacecraft on the lunar orbit under a nearly radial IMF. We found ULF fluctuations (in the plasma rest frame) that can be characterized as a mixture of transverse and compressional modes with different properties at both locations. Moreover we identified both growing and damped waves at the inner spacecraft.

## The Cryo-SA-CRDS Upgrade for a Time Resolved MW Measurement of Electron Number Density

*Shapko D., Dohnal P., Uvarova L., Kassayová M., Roučka Š., Plašil R., Glosík J.*

**Abstract.** The Cryogenic Stationary Afterglow apparatus in conjunction with a continuous wave Cavity Ring-Down absorption Spectrometer (Cryo-SA-CRDS) is a highly sensitive experimental setup for precise study of electron-ion recombination in plasmas in the temperature range of 30-300 K. With the purpose of doing accurate direct measurements of electron number density the microwave diagnostic was newly implemented. The results of the first calibrations and tests will be presented.

## Raysect and Cherab Framework for Diagnostic Forward Modelling

*Tomes M., Bohm P., Sos M., Cavalier J., Martin Imrisek, Fabien Jaulmes, Bogar K., Balner V.*

**Abstract.** Diagnostic operation and design should be supported by intensive modelling to accurately explore the parameter space and output properties. Cherab and Raysect codes form a ray-tracing framework with accurate description of propagation of light rays and plasma radiation. In this contribution its capabilities and application to diagnostic operation and design for the COMPASS and COMPASS Upgrade tokamaks are presented.

## Iron Sulfide Films Prepared for Dye-sensitized Solar Cells

*Tuharin K., Zanáška M., Kudrna P., Tichý M.*

**Abstract.** Abstract: The prospects of iron oxide films and their sulfidation for dye-sensitized solar cells (DSSC) are reviewed. Iron oxide thin films were prepared by hollow cathode plasma jet (HCPJ). The discharge was powered by a constant current source in continuous mode and by a constant voltage source in pulsed mode. Plasma composition was measured by an energy-resolved mass spectrometer. Sulfidation of Iron oxide thin films was performed in the furnace with sulphur vapors. SEM, EDX and Raman spectra of the films are presented. Keywords: hollow cathode plasma jet, iron oxide, iron sulfide, dye-sensitized solar cell

## Comparison of underwater spark simulation using elliptical and cylindrical coordinate systems

*Tuholukov A., Stelmashuk V.*

**Abstract.** For the study of efficiency of underwater spark shock wave generation the simulations of long interelectrode gap discharges are of particular importance. This paper contains descriptions of models of underwater discharge in cylindrical and elliptical coordinate systems and their comparison with experimental data.

## Time Resolved Electron Number Density Measurements in low Temperature Afterglow Plasma

*Uvarova L., Shapko D., Kassayová M., Dohnal P., Plašil R., Roučka Š., Glosik J.*

**Abstract.** The Cryogenic Stationary Afterglow Cavity Ring-Down Spectrometer (Cryo-SA-CRDS) was used to study time evolution of the number density of  $H_3^+$  ions in the afterglow plasma. We used the microwave discharge in He/Ar/H<sub>2</sub> gas mixture to form  $H_3^+$  ions. The aim was to compare the results from the new time resolved electron number density measurement system with the measured  $H_3^+$  ion number density. The results show the transition from  $H_3^+$  dominated plasma to plasma containing both  $H_3^+$  and  $H_5^+$  ions.

## F-3 PHYSICS OF CONDENSED MATTER AND MATERIAL RESEARCH

### NMR Studies of Quadruple Perovskites $\text{SrMn}_7\text{O}_{12}$ , $\text{BiMn}_7\text{O}_{12}$ and $\text{BiMn}_3\text{Cr}_4\text{O}_{12}$

*Adamec M., Chlan V., Kamba S.*

**Abstract.**  $\text{SrMn}_7\text{O}_{12}$ ,  $\text{BiMn}_7\text{O}_{12}$ , and  $\text{BiMn}_3\text{Cr}_4\text{O}_{12}$  are multiferroic quadruple perovskites, undergo several phase transitions and display complex magnetic structures at low temperature. Although the chemical composition is similar, the magnetic structure differs in these systems. We present  $^{55}\text{Mn}$  NMR spectra acquired at low temperatures in wide frequency range for all materials, as well as  $^{53}\text{Cr}$  NMR spectra of  $\text{BiMn}_3\text{Cr}_4\text{O}_{12}$  and in case of  $\text{SrMn}_7\text{O}_{12}$  also temperature and external magnetic field dependences. Assignment of the spectral lines is suggested and possible interpretation is given.

### Tellurite Glasses of the $\text{TeO}_2$ -ZnO-BaO System for Optical Applications

*Hrabovsky J., Desevedavy F., Strizik L., Kalenda P., Wagner T., Smektala F., Veis M.*

**Abstract.** This work deals with a systematic study of optical, structural and thermal properties of the  $\text{TeO}_2$ -ZnO-BaO (TZB) glasses and their ability for doping with  $\text{Er}^{3+}$  ions in order to achieve the 1550 nm Stokes photoluminescence and upconversion photoluminescence emission in visible and near-infrared spectral region. The intensities of  $\text{Er}^{3+}$  intra-4f electronic transitions were calculated on the basis of the Judd-Ofelt theory with derived phenomenological parameters  $\omega_2$ ,  $\omega_4$  and  $\omega_6$  parameters.

## Static and Dynamic Magnetoelectric Coupling in TbMnO<sub>3</sub> Modified by Fe<sup>3+</sup> Substitution

Maia A., Vilarinho R., Mihalik jr. M., Zentková M., Mihalik M., Proschek P., Prokleška J., Kadlec C., Kadlec F., Kamba S., Almeida A., Agostinho Moreira J.

**Abstract.** One of the best known multiferroics is TbMnO<sub>3</sub>, where the emergence of a ferroelectric polarization is described in the framework of the Dzyaloshinskii-Moriya interaction between nonparallel spins. Dynamical magnetoelectric (ME) effects have been identified in the form of electromagnons, i.e., magnons excitable by an electric field. Rare-earth manganites are known to exhibit a strong coupling between magnetism and lattice, which can be manipulated to tailor their physical properties. Previous studies in TbMnO<sub>3</sub> ceramics show that the substitution of Mn<sup>3+</sup> by small amounts of the identically sized Fe<sup>3+</sup> ion profoundly alters the ME coupling. Since these studies were done in ceramics, anisotropic effects could not be ascertained. In this work, the temperature and magnetic field dependence of the ME properties of oriented single crystals of TbMn<sub>1-x</sub>Fe<sub>x</sub>O<sub>3</sub> with  $x = 0.02$  and  $0.04$  were studied. It was found that the presence of Fe<sup>3+</sup> has a striking impact in the ME coupling, modifying the magnetic field dependence of the electric polarization and the electromagnon spectra. An overview of the main results will be presented, highlighting the contrast with previously reported studies on TbMnO<sub>3</sub>.

## GW Approximation for *ab-initio* Calculation of Molecular Transport

Marek Š., Korytár R.

**Abstract.** In order to calculate the transport properties of molecular junctions, extended molecules which include parts of the electrodes need to be investigated. However, such systems are too large to be solved by direct quantum mechanical calculation. Instead, DFT framework is often used. But, since DFT is a ground state theory in its nature, it fails to account for certain transport phenomena. The GW approximation extends the DFT framework so that excitation phenomena is included.



## Generation and Detection of Quantum Turbulence in He II by Second Sound

*Midlik Š., Schmoranzer D., Skrbek L.*

**Abstract.** We report a study of quantum turbulence in superfluid helium generated by a high amplitude wave of temperature (second sound) in a closed square-cylinder resonator. We have investigated steady state turbulence at multiple temperatures, generated using 3 different resonant modes. The amount of quantized vortices was determined from the attenuation of low amplitude second sound oriented transversally. The goal of this work is to identify the parameters describing the onset of flow instabilities.

## Incorporation of A2B6 Quantum Dots Inside Solid-State Matrices

*Vorontsov D., Fučíková A., Valenta J.*

**Abstract.** In this work charge-driven incorporation of CdTe/CdS and CdS quantum dots inside potassium dihydrogen phosphate crystals is shown, as the photophysical and structural properties of obtained composites are thoroughly investigated. In addition, the impact of the matrix on the photostability and thermal sensitivity of incorporated quantum dots was studied and compared for cases of calcium carbonate, potassium bromide and barium sulfate as the host matrices.

## F-4 BIOPHYSICS, CHEMICAL AND MACROMOLECULAR PHYSICS

### Kinetics of Cubic Ice Formation During Cooling of Monoolein/Hemoglobin/Salt/Water System

*Baranova L, Angelova A., Shepard W., Andreasson J., Angelov B.*

**Abstract.** Studies of the dynamics of lipid/protein/salt/water biomimetic systems under cryocooling conditions are important both for understanding the factors affecting the curvature of membranes and for controlling and understanding the organization of protein crystals in membrane systems. Ice formation can play a crucial role in these processes. Despite the fact that there are many thermodynamic investigations of the formation of ice crystals in pure water, the crystallization of water in mixtures has been poorly studied. In the present work, we investigated the kinetics of ice formation in a hemoglobin/monoolein/salt/water LCP system by XRD under continuous flow of liquid nitrogen fluid (cryo-streaming). It was shown that first ice crystals of the cubic phase were formed, and after that hexagonal ice crystals appeared. The kinetic curves of cubic ice formation are presented. Acknowledgement: This work was supported by the project Advanced research using high intensity laser produced photons and particles (CZ.02.1.01/0.0/0.0/16\_019/0000789) from European Regional Development Fund (ADONIS).





## Accurate Molecular Dynamics Simulations of Hydrogen-Bonded Condensed-Phase Systems: Theory and Applications

***Březina K.***

**Abstract.** Hydrogen-bonded networks are found in fundamentally important molecular systems such as proteins, nucleic acids, or liquid water. These, and many other systems, have been theoretically studied using simulations of molecular dynamics which provide insight into their microscopic structure and dynamics. However, an accurate and transferable simulation methodology that produces results consistent with experiments requires a quantum treatment of both the electrons and nuclei alike, since nuclear quantum effects can be considerable on the light nuclei of hydrogen atoms. Here, we discuss the theory basics behind the state-of-the-art methods designed for this purpose, including classical ab initio molecular dynamics (AIMD) and path integral quantization of classical nuclei. A combination of these approaches tends to yield high quality results, but can lead to a high computational cost. Methods designed to alleviate these computational requirements are thus discussed accordingly. To showcase an application, we present our recent findings based on AIMD simulations of an unusual hydrogen-bonded system important in organic chemistry: liquid ammonia solution of the benzene radical anion.

### 3D Hepatic Cell Culture Response to Laser Irradiation

***Ertús A., Smolková., Uzhytchak M., Lunova M., Petrenko Y., Kubinová Š., Dejneka A., Lunov O,***

**Abstract.** Utilization of light in medicine started at the beginning of the 20<sup>th</sup> century. Since then, the field of Photobiomodulation was established and nowadays provides some beneficial effects such as tissue reparation, pain relief and reduce inflammation. So far, molecular mechanism of action on living cells remains unclear. Using Low-Power laser irradiation and mammalian hepatic cell lines cultured in 3D conditions, we study interaction between light and living cells. In comparison with traditional 2D cell culture, cells in 3D environment mimics in vivo settings better.



## Gold/Fluorocarbon Nanocomposites for Enhanced Solar-driven Water Evaporation

***Khomiakova N., Krtouš Z., Solař P., Kylián O.***

**Abstract.** The sun is a renewable energy source that can be used to solve many energy and water scarcity problems. However, the efficiency of conventional solar-based desalination decreases dramatically with increasing water volume due to heat loss to bulk water. This principal limitation may be, however, overcome by using light-to-heat conversion materials floatable on the water that concentrate the generated heat to the water surface and thus accelerate the water evaporation. In this study, we investigated the possibility to produce such material by a plasma-based technique that combines a gas-phase synthesis of Au nanoparticles and RF magnetron sputtering of fluorocarbon films on a conventional gauze. It is shown that such produced system is not only floatable on a water surface, but it also enhances the water evaporation rate, i.e. fulfils two basic demands on a new generation of nanomaterials for effective solar-driven evaporation.

## Various Approaches to Preparation (P)LA-Like Plasma Polymer Thin Films

***Krtouš Z., Kousal J., Kuchakova I., Nikiforov A., Ali-Ogly S., Kolářová Rašková Z., Sedlaříková J., Hanyková L., Krakovský I., Lehocký M.***

**Abstract.** Thin films based on polylactic acid have been prepared by different plasma polymerisation approaches. Plasma-assisted vacuum thermal deposition, magnetron sputtering and plasma jet deposition techniques were used under varying discharge power. Prepared layers were characterized in terms of chemical composition (XPS, NMR and FTIR) and structural homogeneity. Further we investigated the degradability of the films and their wash-off behavior was monitored. The properties of the films were found to be tunable by the deposition conditions to a significant degree.

## Drop Coating Deposition Raman Spectroscopy of Biologically Important Molecule

*Kuižová A., Kuzminova A., Kylián O., Procházka M., Kočíšová E.*

**Abstract.** Drop Coating Deposition Raman (DCDR) method is based on the deposition of a droplet (several microliters) of a solution or suspension on a hydrophobic substrate. Evaporation of the droplet often leads to the formation of a ring pattern known as "coffee ring" effect. The final shape of the deposit, from which Raman spectra are acquired, is influenced by the properties of the substrate (hydrophobicity, roughness) and sample (volume, concentration). DCDR technique enables to measure the samples of solutions at low initial concentrations and small volumes as well. In our research, we focus our attention on two different samples – suspensions of liposomes and solutions of contaminants. As for liposomes, we studied a drying process on non-commercial hydrophobic substrates with different roughness. We showed that for liposomes, increasing roughness of the substrate leads to better preconcentration of initial suspension, thus to the higher intensity of the Raman spectra. Focusing on contaminants, we are trying to find DCDR detection limits using a smooth commercial hydrophobic substrate SpectRIM™ (Tienta Sciences).

## Core@Shell Ag@Ti Nanoparticles Prepared by In-flight Coating

*Libenská H., Hanuš J., Ahadi A. M., Kudrna P., Cieslar M., Košutová T., Kylián O., Červenková V., Biederman H.*

**Abstract.** Heterogeneous nanoparticles are of great potential due to their physical, optical, chemical or catalytic properties of used materials. Different types of NPs as dumbbell, Janus, satellite, core@shell and others can be fabricated. This study is focused on a system preparing core@shell (Ag@Ti) NPs by fully vacuum plasma-based method. Silver nanoparticles were produced in a gas aggregation source (GAS) of Haberland type and in-flight coated by sputtering of titanium targets from two magnetrons.



## Quantification of Triplet excitons Photogenerated by Singlet Fission in bis(furanyl)diketopyrrolopyrroles

*Thottappali M. A., Rais D., Pauk K., Imramovský A., Vala M., Marková A., Pflieger J.*

**Abstract.** Photophysical phenomena of thin films of diketopyrrolopyrrole (DPP) derivatives with furan groups in 3,6 positions and various alkyl groups attached in the N, N' positions were studied using ultrafast transient absorption spectroscopy. Fast conversion of excited states into long-living states with a simultaneous increase of the ground state bleach was observed. It suggests that triplet states are formed by singlet fission. Using a singlet depletion analysis, we found yield of the process exceeding 100 percent for hexyl substituted DPP.

## F-5 PHYSICS OF SURFACES AND INTERFACES

### Ir-Decorated Pt Nanoparticles for Oxygen Evolution and Reduction Reactions

*Blanco Redondo L., Matolín V., and Lobko Y.*

**Abstract.** In this study, Pt nanoparticles decorated with Ir have been produced by polyol method with various compositions (Pt90%Ir10%, Pt80%Ir20%, and Pt60%Ir40%). In addition, polyvinylpyrrolidone (PVP) has been added as capping agent to prevent agglomeration and to decrease the average particle size. The samples have been characterized via Rotating Disk Electrode (RDE) technique, X-Ray Photoelectron Spectroscopy (XPS), and Transmission Electron Microscopy (TEM), and X-Ray diffraction (XRD).

### Characterization of Thermally Expanded Graphite for Polymer Composites' Bipolar Plates for PEM Fuel Cells

*Darabut A. M., Lobko Y., Matolín V.*

**Abstract.** Nowadays, proton exchange membrane fuel cells (PEM FCs) is used as an alternative power source either in stationary or mobile applications. The bipolar plates (BPs), one of the critical components of the PEM FCs, must provide specific requirements to accomplish the best performance. The polymer composites' BPs are one of the most promising materials, owing to the good mechanical properties, high electrical and thermal conductivity, etc., in comparison to other materials such as graphite or metal. The polymer composites are formed from two parts, the matrix (epoxy resin) gives the mechanical properties, and the carbon fillers (graphite, carbon black, etc.) supply the conductivity. The thermally expanded graphite is natural graphite modified by a chemical and thermal process, which allows the expansion of the interlayer and the formation of pores. The influence of the expansion temperature on the morphology of TEG was investigated by SEM and TEM. The thermally expanded graphite was characterized by XPS, EDS, FTIR and Raman spectra, and BET surface area analysis. Finally, the TEG obtained was compared with commercial graphite in terms of electrical conductivity.

## Adsorption of Phenylphosphonic Acid on Cerium Oxide Surfaces with Different Stoichiometry

*Kalinovych V., Kosto J., Piliai L., Prince K. C., Matolín V., Matolínová I., Skála T., Tsud N.*

**Abstract.** The adsorption geometry and thermal stability of phenylphosphonic (PPA) acid on cerium oxide surfaces with different stoichiometry ( $\text{CeO}_2$ ,  $\text{CeO}_{1.7}$ ,  $\text{Ce}_2\text{O}_3$ ) were studied. The investigation was carried out using synchrotron radiation based photoemission techniques and near edge X-ray absorption fine structure spectroscopy. The PPA molecules adsorb intact on the surface at 25 C independently of the oxide stoichiometry. The thermal treatment causes the decomposition of the PPA adlayer via P-( $\text{C}_6\text{H}_5$ ) bond scission.

## Ethanol Sensing Mechanism of ZnO Nanorods Based Chemiresistor Studied by NAP-XPS

*Vorokhta M., Piliai L., Khalakhan I., Nováková J., Yatskiv R., Grym J., Matolínová I.*

**Abstract.** ZnO nanomaterials are widely used to fabricate efficient gas sensors for the detection of various gases with trace concentrations. In this work the ZnO nanorods based sensor was investigated in presence of  $\text{O}_2$  simulating the ambient air atmosphere,  $\text{O}_2$ /ethanol,  $\text{O}_2$ /ethanol/ $\text{H}_2\text{O}$  and  $\text{O}_2$ /acetaldehyde mixtures by near ambient pressure X-ray photoelectron spectroscopy. Results of this investigation bring new insights towards the ethanol sensing mechanisms of ZnO nanorods based chemiresistor

## Thermal Stability Study of Mixed $\text{CeO}_x\text{-Co}_3\text{O}_4$ Thin Film Oxide Catalysts

*Uvarov V., Fusek L., Krutel J., Mysliveček J., and Johánek V.*

**Abstract.** Thermal stability of mixed  $\text{CeO}_x\text{-Co}_3\text{O}_4$  thin films is investigated for a model system of non-continuous cerium oxide supported on  $\text{Co}_3\text{O}_4(111)/\text{Ir}(100)$  and on oxidized polycrystalline cobalt. Stepwise thermal annealing under UHV was monitored by X-ray photoelectron spectroscopy (XPS) and microscopy (STM or SEM). There is a temperature dependent interplay between cerium and cobalt oxides via oxygen transfer. The thermal reduction of the model system is significantly less intensive than for the highly corrugated layer on Co.



## Pt-CeO<sub>2</sub>-C Thin Film Catalyst Prepared by Magnetron Co-sputtering for Proton Exchange Membrane Fuel Cells

*Xie X., Yakovlev Y., Kúš P., Nováková J., Matolínová I., Khalakhan I.*

**Abstract.** In order to decrease the Pt-loading and develop a high-performance catalyst for PEMFCs, the Pt-C-CeO<sub>2</sub> thin film catalyst was prepared by magnetron co-sputtering in Ar+O<sub>2</sub> atmosphere. The CeO<sub>2</sub> and C are used for a dopant to increase the porosity and metal support to maintain the particle size during the degradation process, respectively, resulting in a significant improvement of ORR activity. The electrochemistry properties of Pt-C-CeO<sub>2</sub> thin film catalyst was measured in RDE (half-cell), shows higher ECSA and mass activity in comparison with Pt. The new catalyst was applied in MEA (single-cell) to further prove the applicability, which provides greater specific power density than Pt. Additionally, Pt-C-CeO<sub>2</sub> catalyst possesses better durability during ADT procedure in half cell and single cell. The change of catalyst microstructures and composition were characterized by SEM, XRD, TEM, XPS, and EDX.

## F-6 QUANTUM OPTICS AND OPTOELECTRONICS

### Evaluation of Charge Transport Properties in Perovskite Radiation Detectors

***Brynza M., Musiienko A., Belas E., Pipek J., Praus P., Ahmadi M., and Grill R.***

**Abstract.** Currently, solar cells based on hybrid organic-inorganic perovskites are being actively studied. Perovskites have several potentially useful physical properties for generating electricity from the sun. Non-radiative recombination remains the main factor limiting the efficiency of perovskite optoelectronic devices. In this study, we aim to find the recombination pathways and to reveal interactions between traps and free carriers in MAPbBr<sub>3</sub> by time-of-flight (ToF) current spectroscopy and Monte Carlo simulation. The knowledge of defect structure can lead to the development of more effective perovskite devices.

### Arrays of Single-Photon Detectors in Boson Sampling Schemes

***Byelova M., Len V., Semenov A.***

**Abstract.** Boson sampling is a non-universal quantum algorithm for computing matrix permanents. We have adapted this scheme for realistic photodetection by an array of single-photon detectors. The consideration is based on the corresponding photocounting equation. We have derived a technique for reconstruction of permanents with such detectors. We believe that our result will be useful for practical implementations of optical non-universal quantum computers.

### Laser Spectroscopy of Antiferromagnets

***Kimák J., Wohlrath V., Kubaščík P., Surýnek M., Schmoranzarová E., Němec P.***

**Abstract.** Antiferromagnetic spintronics attracts significant attention nowadays. Laser spectroscopy and magneto-optics (MO) are powerful tools for investigation of properties of antiferromagnets, such as phase transitions, spin dynamics, internal structure, etc. We studied optical and MO properties of non-collinear antiferromagnet Mn<sub>3</sub>NiN on STO substrate. We observed that cooling of the sample leads to very strong changes of its reflectivity and MO response which we attributed to substrate-induced strain.



## Time-domain Terahertz Spectroscopy

***Klimovič F.***

**Abstract.** Time-domain terahertz spectroscopy is a powerful tool for investigation of charge transport phenomena. In the last two decades, it has been employed for the study of various semiconductor nanostructures as well as materials like graphene. This contactless method allows for sub-picosecond time resolution of charge carrier dynamics. We will give an overview of theoretical formalism used for the interpretation of terahertz spectra, which is still being discussed.

## Boson Sampling with Dead Time of Detectors

***Len V., Byelova M., Semenov A.***

**Abstract.** The scheme of boson sampling is an example of non-universal quantum algorithms. Its implementation with realistic detectors raises the issue of discriminating adjacent photon numbers. As a solution, we suggest the technique of continuous-wave detection, for which dead time of detectors plays a crucial role. We propose a realistic scheme for implementation of boson sampling with continuous-wave detection, which can be useful for computing matrix permanents with a reasonable time.

## High Harmonic Generation in Solids

***Suthar P., Kozak M.***

**Abstract.** Non-perturbative High Harmonic Generation (HHG) from solids was first reported in ZnO in 2010. Since then HHG has been observed in a number of different crystals, in reflective geometry, from nano-structured solids, and from two dimensional materials. A related but distinct phenomenon is the generation of high order sideband generation in solids. We will try to better understand the physical mechanisms behind these two processes using experiments and theory.

## F-9 PARTICLE AND NUCLEAR PHYSICS

### Detector for Luminosity Measurements at High Energy Physics Experiments

*Barsuk S., Burmistrov L., Bezshyyko O., Golinka-Bezshyyko L., Orlov V., Yeroshenko V.*

**Abstract.** Luminosity measurement detector is a project of fast Cherenkov veto counter for both online and offline analysis applied for operation in p-p collisions, beam-gas, and heavy-ion modes. We performed a Geant4 simulation of the quartz detector using events generated by Pythia8 to study various options to optimize luminosity measurement precision. Several different geometries and configurations were proposed and simulated using the Geant4 framework.

### Isomer Ratios for Products of Photonuclear Reactions on Ag

*Bezshyyko O. A., Golinka-Bezshyyko L. A., Kadenko I., Kotenko A. V., Povar T. V., Vodin O., Kushnir V., Mitrochenko V., Olejnik S., Perezhogin S. A., Lysenko V. S.*

**Abstract.** Experimental measurements and calculations of isomer ratios for the products of photonuclear reactions on silver with escape of several particles were performed with application of bremsstrahlung with 43.4 MeV endpoint energy. Argentum targets with natural composition to study the reaction  $^{107}\text{Ag}(\gamma, 3n)^{104\text{m,g}}\text{Ag}$  were irradiated. The LU-40 linear electron accelerator was used as the source of bremsstrahlung radiation. The HPGe spectrometer (with efficiency 20 % and an energy resolution 1.9 keV for the 1332 keV  $^{60}\text{Co}$  line) was applied for measurement of gamma spectra.

### Commissioning of Truebeam Linear Accelerator

*Fedorova A., Alokina M.*

**Abstract.** Commissioning is a necessary and important step which must be done for appropriate clinical usage of a medical equipment for radiotherapy. Goal of this work is to investigate and compare beam data measurements for 6MV & 10MV FF (flattening filter) and 6MV & 10MV FFF (flattening filter free) beams obtained on the Truebeam linear accelerator by Varian Medical Systems. Studied parameters are PDD (Percentage Depth Dose), Profiles, Flatness and Symmetry, Penumbra, Leaf Transmission and DLG (Dosimetry Leaf Gap).



## Artificial Intelligence Algorithms in Nuclear Physics, HEP, and Medical Physics

*Natochii A., Bezshyyko O., Golinka-Bezshyyko L., Semkiv N.*

**Abstract.** Artificial Intelligence algorithms provide unmatched reliability and cost-effectiveness for data analysis. They are often used in High Energy Physics and Applied Nuclear Physics. The objective of my work is to study algorithms of AI and their implementation in these fields. The calculations were done on a workstation with two Intel Xeon processors with 96 threads and two Nvidia GeForce RTX 2080 Ti GPUs. The results of this work can be applied to extend AI methods on a broad range of tasks.

## Linearity of Light Yield in JUNO Neutrino Experiment

*Tměj T.*

**Abstract.** The signal from scintillator detector is approximately linear to the deposited energy. Even though it is mostly linear there are some deviations. The knowledge of the nonlinearity is essential for the precise determination of the deposited energy in neutrino experiments using the liquid scintillator such as JUNO, multipurpose neutrino detector with rich physics program containing about 20 kton of liquid scintillator. The presented method of the nonlinearity measurement uses the process of Compton scattering where the gamma rays scatter inside the liquid scintillator. Calibrated HPGe detector measures the energy of the scattered gamma rays with high precision. The signal from the HPGe detector and the known original energy of the gamma particle determine the true value of the deposited energy inside scintillator. The examined nonlinearity is the deviation from the linear dependence of the liquid scintillator signal on the true deposited energy.



## F-11 MATHEMATICAL AND COMPUTER MODELLING

### Collective Variable Search Using Neural Networks

*Šípka M., Grajciar L., Pavelka M.*

**Abstract.** In enhanced sampling methods such as metadynamics, it is crucial to identify so-called collective variables to capture important features of the evolution. The method of using generative neural networks to automatically identify the right variables is a promising new approach, that takes advantage of the network's ability to process a large amount of data and identify few key characteristics.



## F-12 PHYSICS EDUCATION AND GENERAL PROBLEMS OF PHYSICS

### Telescopes in Formal and Informal Education

*Hložek, F.*

**Abstract.** This article presents conclusions from the research of Czech and foreign literature focused on the telescopes' usage in both formal and informal education. The research is presented with surprising conclusion that there is a lack of articles dealing with practical use of telescopes. Collection of ideas and practical uses of telescopes based on the research will lead to creation of teaching materials and models that can develop knowledge and understanding of the concepts of telescopes.



## F-13 PHYSICS OF NANOSTRUCTURES

### Advanced Characterization of Nanomaterials Using Scanning Probe Microscopy

*Cerny M., Fucikova A.*

**Abstract.** Atomic Force Microscopy (AFM) is a powerful imaging technique which provides very high-resolution images and topological data in scales of nanometers. The quality of the obtained data is determined by quality of used AFM tip and fine adjustment of measuring parameters and settings of the machine. The measurement becomes more challenging if the AFM probe is about to approach a soft and elastic surface such as silica gel polymers or biological membrane surfaces. Additionally, in combination with conductive AFM module and Scanning Tunneling Microscopy (STM), we are able to collect data about single Si-NP energetic bands properties.



